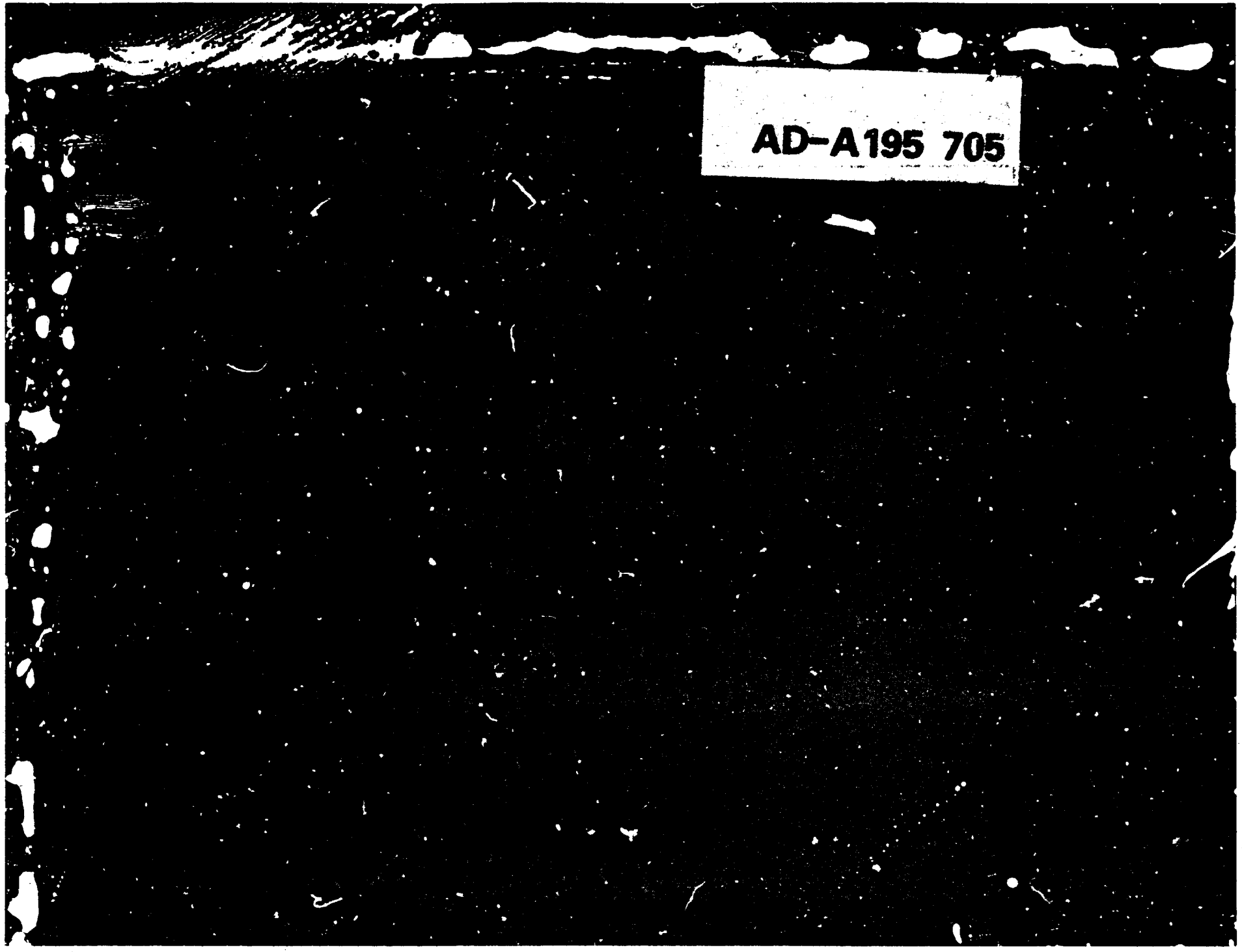
AD-A195 705

UNCLASSIFIED
SECURITY CLASSIFICATION OF THIS PAGE

REPORT DOCUMENTATION PAGE

Form Approved OMB No. 0704-0188

1a. REPORT SECURITY CLASSIFICATION: Unclassified	1b. RESTRICTIVE MARKINGS
2a. SECURITY CLASSIFICATION AUTHORITY	3. DISTRIBUTION/AVAILABILITY OF REPORT
2b. DECLASSIFICATION/DOWNGRADING SCHEDULE	
4. PERFORMING ORGANIZATION REPORT NUMBER(S): BRL-MR-3678	5. MONITORING ORGANIZATION REPORT NUMBER(S)
6a. NAME OF PERFORMING ORGANIZATION: Ballistic Research Laboratory / 6b. OFFICE SYMBOL (If applicable): SLCBR-IB-A	7a. NAME OF MONITORING ORGANIZATION
6c. ADDRESS (City, State, and ZIP Code): Aberdeen Proving Ground, MD 21005-5066	7b. ADDRESS (City, State, and ZIP Code)
8a. NAME OF FUNDING/SPONSORING ORGANIZATION / 8b. OFFICE SYMBOL (If applicable)	9. PROCUREMENT INSTRUMENT IDENTIFICATION NUMBER
8c. ADDRESS (City, State, and ZIP Code)	10. SOURCE OF FUNDING NUMBERS

PROGRAM ELEMENT NO.	PROJECT NO.	TASK NO.	WORK UNIT ACCESSION NO.
62618A	1L162618AH80	00	00

11. TITLE (Include Security Classification)

Studies Supporting Development of a Modified Gradient Equation for Lumped-Parameter Interior Ballistic Codes

12. PERSONAL AUTHOR(S)
F. W. Robbins and G. E. Keller

13a. TYPE OF REPORT	13b. TIME COVERED	14. DATE OF REPORT (Year, Month, Day)	15. PAGE COUNT
Memorandum Report	FROM Oct 1985 TO Oct 1986		

16. SUPPLEMENTARY NOTATION

(computerized)

17. COSATI CODES		
FIELD	GROUP	SUB-GROUP
19	01	
21	02	

18. SUBJECT TERMS (Continue on reverse if necessary and identify by block number)

Gradient, Gradient Equation, Interior Ballistics, Lumped-Parameter

19. ABSTRACT (Continue on reverse if necessary and identify by block number)

Test firings of 120-mm rounds were performed to characterize effects due to the combustible cartridge cases used. Comparisons were made between measured ballistic parameters, especially gas pressures, and those predicted by simulation calculations performed with interior ballistic codes. It was found that the two-phase flow gun code XNOVAKTC (XKTC) modeled the gun firings very accurately. On the other hand, the results of calculations with IBHVG2, a lumped-parameter interior ballistic code, differed significantly from both the measurements and the XKTC calculations. The difference is much larger for systems with large charge-mass-to-projectile-mass (C/M) ratios. Ballistic parameters which affect the pressure gradient, especially for large C/M ratios, are examined in detail. One parameter which is essential to good physical modeling is chambrage, the narrowing of the case mouth of the cartridge; other potentially important parameters are identified. Keywords: Gradient equations. (edc)

20. DISTRIBUTION/AVAILABILITY OF ABSTRACT	21. ABSTRACT SECURITY CLASSIFICATION
☒ UNCLASSIFIED/UNLIMITED ☐ SAME AS RPT. ☐ DTIC USERS	Unclassified

22a. NAME OF RESPONSIBLE INDIVIDUAL	22b. TELEPHONE (Include Area Code)	22c. OFFICE SYMBOL
Frederick W. Robbins	(301) 278-6201	SLCBR-IB-A

DD Form 1473, JUN 86 — Previous editions are obsolete.

SECURITY CLASSIFICATION OF THIS PAGE
UNCLASSIFIED

A

TABLE OF CONTENTS

LIST OF FIGURES

LIST OF TABLES

ACKNOWLEDGMENTS

The authors wish to thank Dr. P. S. Gough for helpful discussions and technical insight, Mr. A. W. Horst for his enthusiastic technical support, Mr. R. D. Anderson for changes made to IBHVG2, and Mr. G. M. Mason for performing many computer runs.

I. INTRODUCTION

In a recent study, 120-mm gun firings were performed to establish the ballistic contributions due to the combustible cases used[1]. Measured velocities and pressures were compared with matching interior ballistic code simulations with the hope of quantifying those contributions. Previously, for firings for which the charge-mass-to-projectile-mass (C/M) ratio was low, IBHVG2, a lumped-parameter interior ballistic code, has provided good comparisons[1,2]. Also in the past, the NOVA family of two-phase interior ballistic codes, of which XNOVAKTC (XKTC) is the latest version, has been shown to be able to simulate firings with very good success[1,2,3,4]. In this recent study, however, for which the C/M was about unity, there was a wide disparity between the predictions of XKTC and those of IBHVG2 for the same nominal data base.

In the previous work[1], it was shown that XKTC could be made to mimic the experimental 120-mm gun firings quite well. For IBHVG2, however, that was not the situation. For one case, IBHVG2 gave a calculated maximum breech pressure that was 42 MPa higher than that predicted by XKTC for the same nominal data base. It was found that a difference of 14 MPa could be attributed to the fact that IBHVG2 does not model the projectile boattail intrusion, and that 3 MPa each could be attributed to the fact that IBHVG2 neither models flamespreading nor intergranular stress. The major difference in the predicted maximum pressures, however, was attributed to the simple physics used in the derivation of the pressure gradients allowed by IBHVG2. In XKTC, the axial pressure gradient is calculated from first principles and analytic correlations; in IBHVG2, only analytical pressure gradient relations due to Lagrange and due to Pidduck-Kent[5] are available.

In this report, several ballistic parameters which might affect the pressure gradient, especially for large C/M ratios, are examined in some detail. The objective of this study was to determine the physics that must be included in the analytic gradient equation, so that the predictions of lumped-parameter codes can be improved.

II. INITIAL COMPARISONS BETWEEN EXPERIMENT AND XKTC

The 120-mm experimental gun firings are described in a previous paper[1]. The gun tube was instrumented with five pressure gages in the chamber: two at 95 mm, one at 286 mm (midchamber) and two at 489 mm from the rear face of the tube. There were also seven downbore gages, situated at 768 mm, 1048 mm, 1530 mm, 2292 mm, 3054 mm, 3816 mm, and 4578 mm from the rear face of the tube. Assuming that the gages at 95 mm determine the breech pressure accurately, that the base of the projectile before it moves is located at 541 mm from the rear face of the tube, and that the pressure measured as each downbore gage is uncovered is the projectile base pressure at that time, one can use the data contained in Reference 1 to calculate the ratio of the breech pressure to the projectile base pressure for several discrete values of projectile travel. Table 1 presents the average pressure ratios for the three gun firings which were performed with no cases and average pressure ratios for the three gun firings which were performed with inert cases.

Table 1. Experimental Ratios of Breech Pressure to Projectile Base Pressure at Several Discrete Values of Projectile Travel

Travel (m)	0.227	0.507	0.989	1.751	2.513	3.275	4.037
No case	1.33	1.40	1.61	1.65	1.39	1.49	1.65
Inert case	1.29	1.35	1.64	1.70	1.46	1.51	1.65

The data points for the ratios of the breech to projectile base pressure versus travel from Table 1 are plotted against calculated curves of these ratios from XKTC in Figure 1. Both the caseless gun firing series and the inert case gun firing series are shown. Breech and base pressure curves are added to assist in interpreting the ratio data. The XKTC calculations were performed using measured values wherever possible and reasonable values for all other input data. These simulations gave excellent agreement with measured pressure-time curves and pressure difference curves. The agreement between the measured values and the calculated values for pressure ratios for all but the last two points is very good. The reason for the last points not fitting well is not known. In any case, this good agreement, at least for the major portion of the ballistic event, should make XKTC a useful tool for studying the gradient phenomenology. With this understanding, in this report, XKTC calculations have been assumed to furnish the "correct" answers with which to compare lumped-parameter calculations.

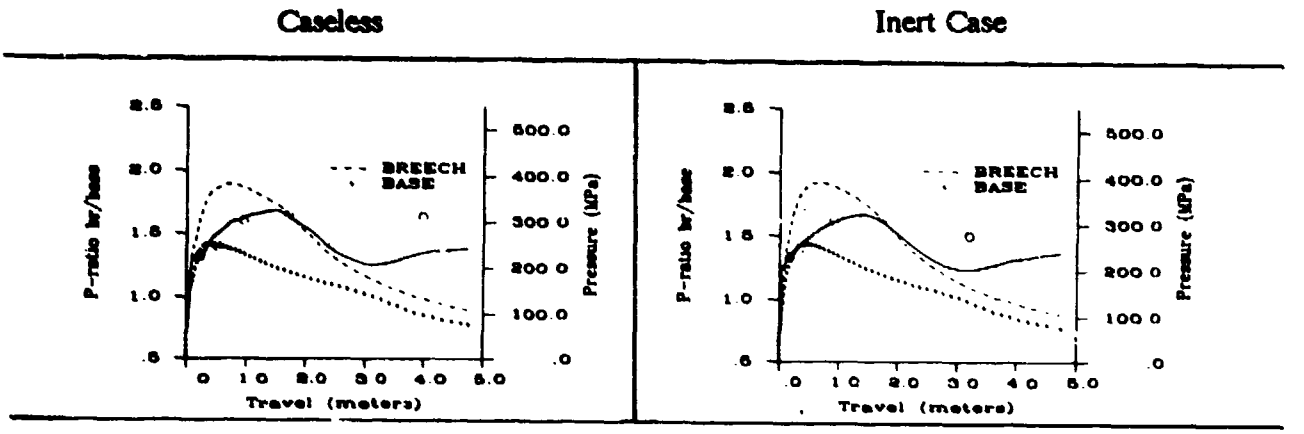

Figure 1. Comparisons Between Measured and XKTC-Calculated Ratios of Breech Pressure to Base Pressure.

III. FIRST MODEL COMPARISONS

As we have shown that that XKTC could be used for accurate simulations of gun firings, we sought to perform calculations with XKTC specifically simplified so that IBHVG2 calculations could be compared to them. To that end, the first series of calculations performed with XKTC utilized data bases with (a) 7-perforated granular propellant evenly distributed along the length of the chamber, (b) the chamber diameter equal to the bore diameter, (c) zero barrel resistance, (d) a flat-based projectile, (e) nominal heat loss to the chamber walls, and (f) a

propellant ignition temperature equal to the ambient temperature, so that the propellant was all ignited at the start of calculations. A typical XKTC data base used in this study is included as Appendix A. The companion IBHVG2 data base is included as Appendix B.

Guns with two different chamber volumes were simulated, one with a chamber volume of 9832.2 cm^3 and one with a chamber volume of 98.322 cm^3. Two different guns were simulated in order to determine whether the observed effects were a function of the physical size of the weapon. The other weapon parameters that were associated with each of these two guns are are shown in Table 2. For each of the two weapons, two different projectile weights were used to produce the two different C/M ratios for which calculations were performed.

Table 2. Weapon Parameters for the First Series of Calculations

Chamber volume	9832.2 cm^3	98.322 cm^3
Travel	4.572 m	1.88 m
Propellant mass	9.8 kg	0.098 kg
Projectile masses	9.8 kg and 39.2 kg	0.098 kg and 0.392 kg
Bore diameter	127.0 mm	28.65 mm

The effects of propellant burn rate and the maximum chamber pressure were also examined. Table 3 shows the parameters which were varied:

Table 3. Other Parameters for the First Series of Calculations

Burning Rate (p in MPa)	1.10519 $p^{1.0}$ mm/s		0.408451 $p^{0.8}$ mm/s
Max Pressure	172 MPa	345 MPa	517 MPa

The propellant thermochemistry for all calculations is shown in Table 4.

Table 4. Propellant Thermochemistry

Impetus	1136 J/g
Covolume	0.976 cm^3/g
Gamma	1.23
Flame Temperature	3141 K
Molecular Weight	23.0 g/g-mole
Density	1.66 g/cm^3

Table 5. Comparisons of Calculated Maximum Breech Pressures and Muzzle Velocities for XKTC and IBHVG2

			XKTC				IBHVG2							
							Lagrange Gradient				Pidduck-Kent Gradient			
Ch Vol	BR	C/M	Maximum Breech Pressure (MPa)	Time (ms)	Muzzle Velocity (m/s)	Time (ms)	Maximum Breech Pressure (MPa)	Time (ms)	Muzzle Velocity (m/s)	Time (ms)	Maximum Breech Pressure (MPa)	Time (ms)	Muzzle Velocity (m/s)	Time (ms)
L	1.0	1.0	173	7.7	957	13.3	183	7.5	966	13.3	179	7.5	963	13.3
L	1.0	1.0	345	6.5	1352	10.4	346	6.3	1363	10.3	337	6.3	1356	10.3
L	1.0	1.0	517	6.1	1594	9.1	496	5.9	1559	9.1	481	5.9	1561	9.1
L	1.0	0.25	174	13.8	549	23.7	179	13.5	557	23.5	179	13.5	557	23.5
L	1.0	0.25	345	11.2	779	18.1	348	11.1	783	18.0	348	11.1	783	18.0
L	1.0	0.25	518	10.4	887	15.9	518	10.3	891	15.8	516	10.3	892	15.8
L	0.8	1.0	172	4.7	894	11.2	184	4.7	892	11.2	181	4.6	894	11.2
L	0.8	1.0	347	3.8	1250	8.2	363	3.6	1260	8.2	357	3.6	1261	8.2
L	0.8	1.0	517	3.4	1494	6.9	530	3.0	1487	6.9	522	3.1	1492	6.9
L	0.8	0.25	177	8.3	511	19.8	179	8.3	515	19.7	179	8.3	515	19.7
L	0.8	0.25	343	6.5	710	14.6	345	6.5	718	14.6	344	6.5	718	14.6
L	0.8	0.25	514	5.5	850	12.2	518	5.6	856	12.2	516	5.6	856	12.2
S	1.0	1.0	172	1.4	1130	3.5	185	1.4	1083	3.6	183	1.4	1091	3.6
S	1.0	1.0	341	1.2	1552	2.7	343	1.2	1511	2.7	334	1.2	1509	2.7
S	1.0	1.0	516	1.1	1756	2.3	512	1.0	1706	2.3	498	1.0	1710	2.3
S	1.0	0.25	172	2.6	642	6.3	179	2.5	630	6.3	179	2.5	630	6.3
S	1.0	0.25	345	2.1	895	4.7	347	2.1	881	4.7	347	2.1	880	4.7
S	1.0	0.25	518	1.9	987	4.1	513	1.9	975	4.1	513	1.9	975	4.1
S	0.8	1.0	172	.90	1057	3.2	184	.91	1031	3.2	182	.90	1033	3.2
S	0.8	1.0	341	.70	1461	2.3	358	.70	1443	2.4	353	.70	1466	2.4
S	0.8	0.25	172	1.6	590	5.7	175	1.6	587	5.7	174	1.6	587	5.7
S	0.8	0.25	345	1.3	842	4.1	347	1.3	834	4.1	347	1.3	834	4.1
S	0.8	0.25	514	1.1	956	3.5	516	1.1	949	3.5	515	1.1	949	3.5

The comparison calculations performed with XKTC and with IBHVG2 (using the Lagrange gradient model and the Pidduck-Kent gradient model) are summarized in Table 5 for the variations described above. In the table, the "Ch Vol" is the chamber volume of the particular weapon, and "BR" is the propellant burning rate, where "1.0" implies 1.10519 $p^{1.0}$ mm/s and "0.8" denotes 0.408451 $p^{0.8}$ mm/s. The maximum breech pressure and muzzle velocity with their associated times are given in the table. For each horizontal line on this table, the propellant web in the XKTC calculation was varied until the desired peak pressure was achieved; the propellant length was maintained between 2 and 3 times the outer propellant diameter. Then, with the same final propellant dimensions, the associated IBHVG2 Lagrange and the

IBHVG2 Pidduck-Kent calculations were performed.

Close inspection of this table reveals that IBHVG2 agrees with XKTC very closely when C/M is 0.25, for both the Lagrange gradient and the Pidduck-Kent gradient, for both weapons and for both propellant burn rates. However, when C/M is 1.0, agreement is not as good.

This first comparison series of calculations with XKTC and IBHVG2 investigated the influence of C/M, chamber volume, propellant burning rate and maximum breech pressure on ballistic performance. Figures 2 through 5 have been generated from XKTC calculations for the weapon with the large chamber volume. Figure 2 shows plots of the mean to projectile base pressures for C/M equal to 1.0, for increasing maximum breech pressures, and for different burning rates. Figure 3 shows plots of the breech to mean pressure ratios for C/M equal to 1.0, for increasing maximum breech pressures, and for different burning rates. Figure 4 shows plots of the mean to projectile base pressures for C/M equal to 0.25, for increasing maximum breech pressures, and for different burning rates. Figure 5 shows plots of the breech to mean pressure ratios for C/M equal to 0.25, for increasing maximum breech pressures, and for different burning rates. In each of these figures, the plots on the left have increasingly higher maximum breech pressures and were performed with a burning rate of $1.10519\ p^{1.0}$ mm/s, while the plots on the right have the same increasingly higher maximum breech pressures and were performed with a burning rate of $0.408451p^{0.8}$ mm/s. The shape and magnitude of the plots for the smaller chamber volume were the same for the corresponding C/M, burning rates and pressures except the time scale and travel scale were about 1/3 that of the larger chamber volume calculations, so they have not been included in this report. As an aid in interpreting the ratios, the base and breech pressures are plotted on each graph.

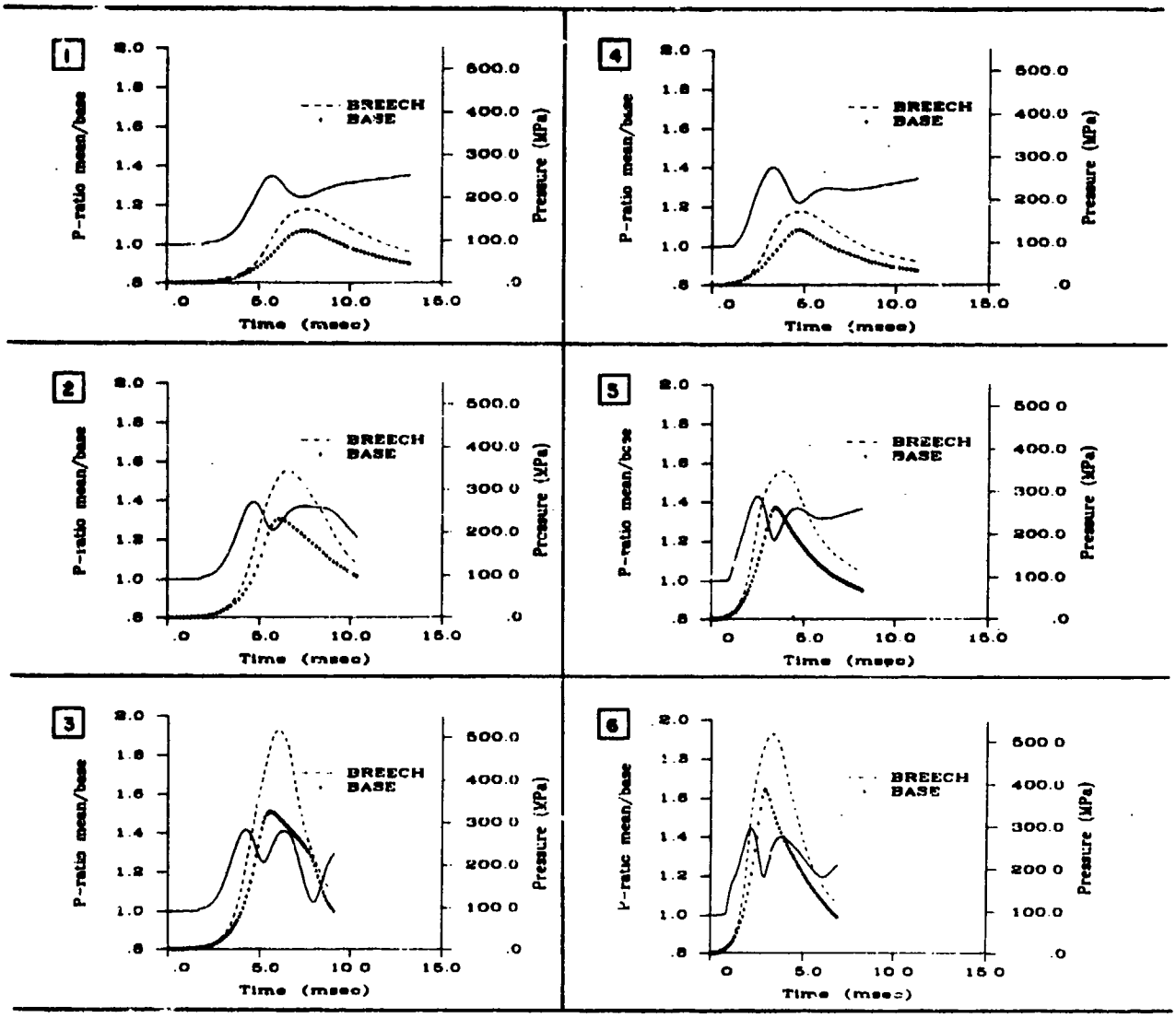

Figure 2. XKTC-Calculated Mean/Base Pressure Ratio Curves for a C/M of 1.0

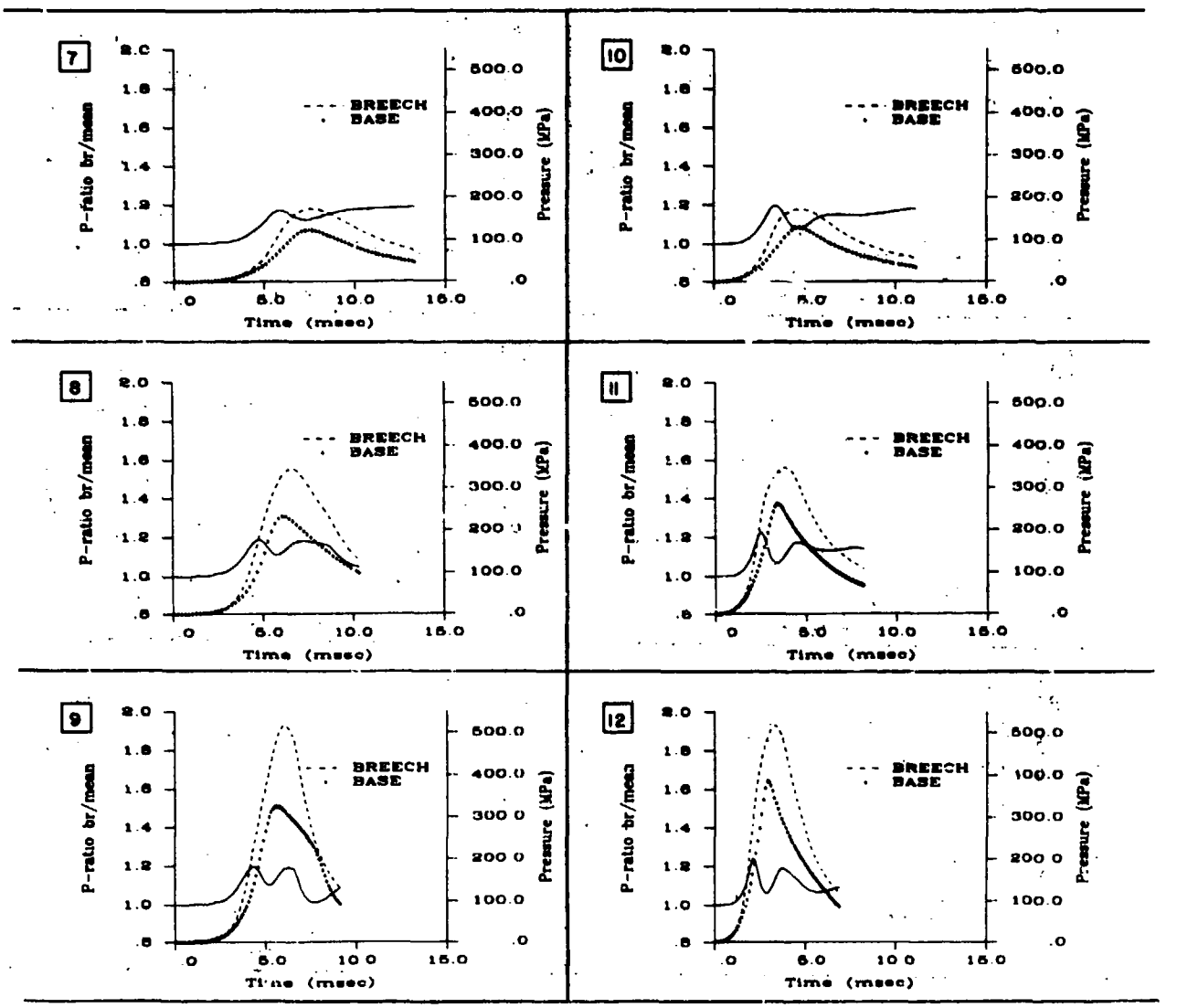

Figure 3. XKTC-Calculated Breech/Mean Pressure Ratio Curves for a C/M of 1.0

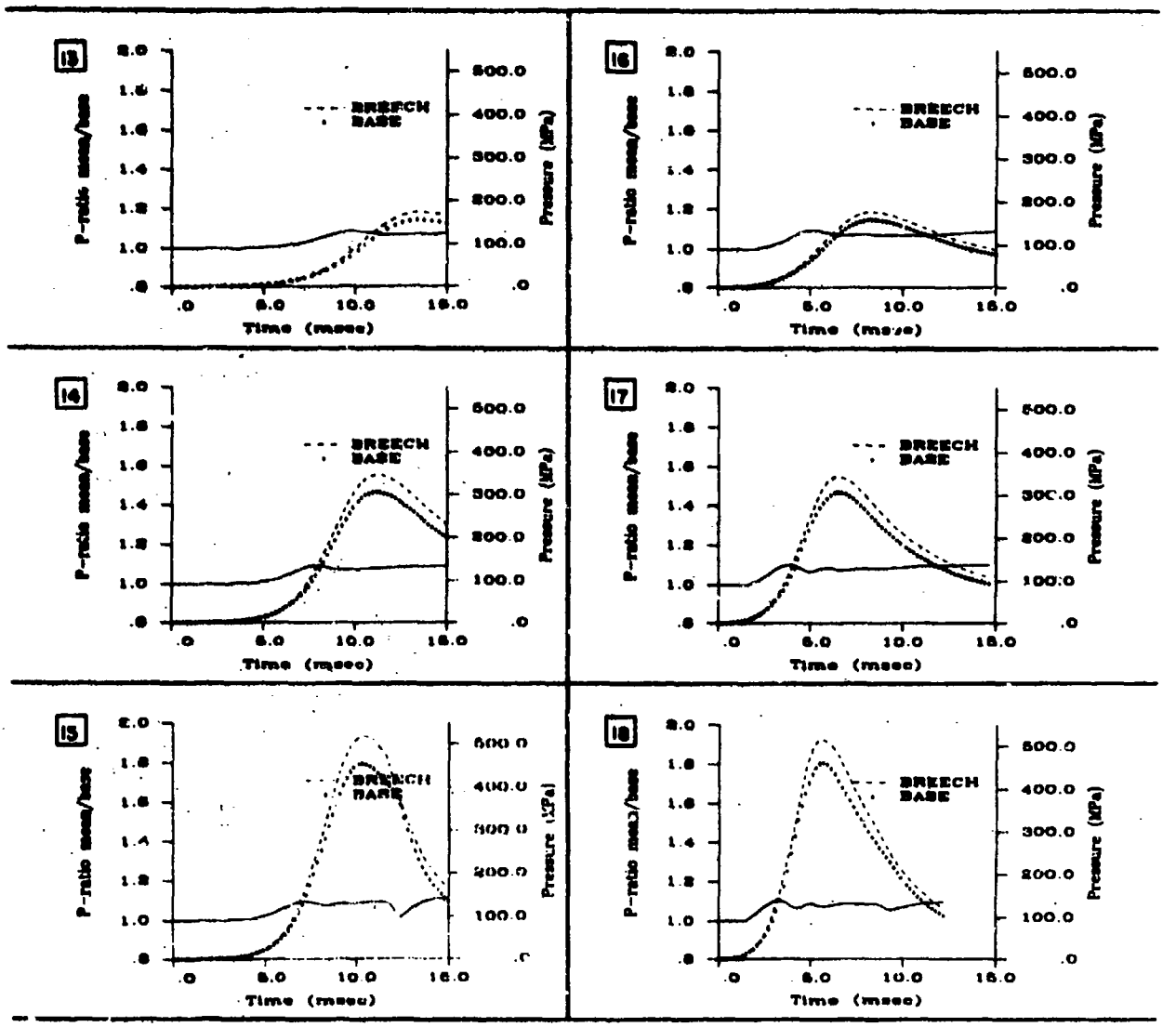

Figure 4. XKTC-Calculated Mean/Base Pressure Ratio Curves for a C/M of 0.25

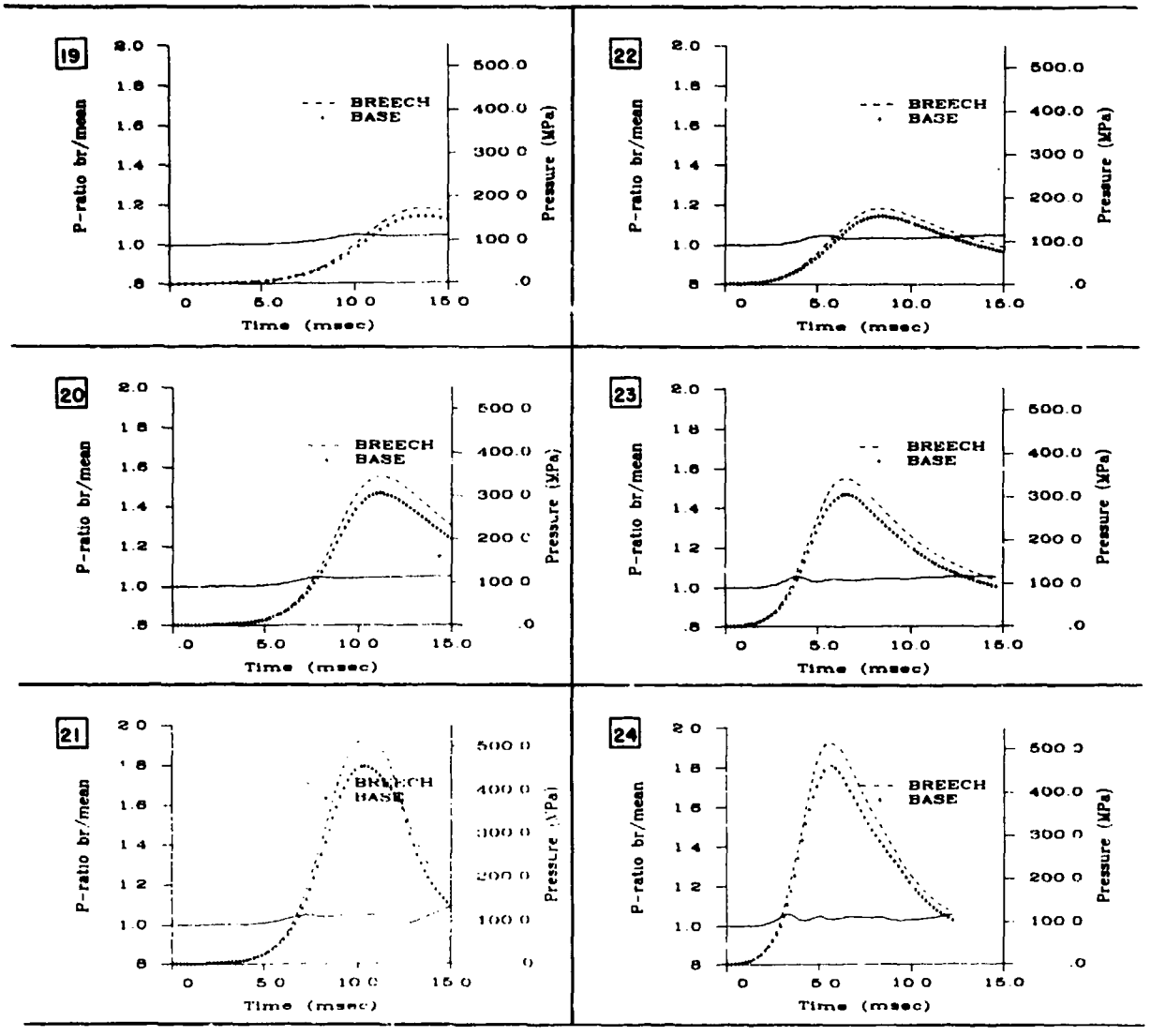

Figure 5. XKTC-Calculated Breech/Mean Pressure Ratio Curves for a C/M of 0.25

The ratio plots in Figures 2 through 5 illustrate the complex nature of the relationship between the breech, mean and base pressures. The general nature of the ratio curves is to be constant near 1.0 for some length of time, followed by a first rise, a drop-off, a second rise and in some cases a second drop-off and another rise. The second drop-off seems to be caused by

the slivering phase of the propellant burning, as it occurs just as XKTC indicates that slivering is taking place. Further, for low pressure calculations, for which the propellant does not sliver before projectile exit, the second drop-off does not occur. Calculations done with a single perforation grain also did not show a second drop-off. The first rise and drop-off may be caused by the rarefaction wave caused by the projectile motion, the first peak corresponding to the time that the rarefaction wave reaches the breech face and the first minimum corresponding to the time the reflected wave reaches the base of the projectile. In all of these XKTC calculations, we observed that an ullage region opens up between the projectile base and the front end of the propellant bed. In this ullage region, the pressure drop per unit of distance across this ullage region is much smaller than across the propellant bed. Gough[5] has speculated that the formation of an ullage region, as observed in the XKTC calculations, and the dircontinuity in gas velocity at the propellant/ullage boundary may contribute to the undulatory shape of the mean to base pressure ratio.

There remained the question, however, of what physical processes were responsible for the greater than 10% maximum breech pressure differences observed between real-world simulations with XKTC and the equivalent IBHVG2 calculations, the differences that motivated this study.

IV. SECOND MODEL COMPARISONS

The second set of model comparisons included calculations at both high and low C/M, because C/M was implicated in the lack of agreement between XKTC and IBHVG2 in the first comparisons. The Lagrange gradient was used for all IBHVG2 calculations. Several other parameters were also varied to determine their contribution to the problem. For these calculations, we modeled the weapon with the 9832.2 cm^3 chamber volume, and we used a burning rate exponent of 1.0. We varied the barrel resistance for both XKTC and IBHVG2 calculations, and for XKTC, introduced flamespreading and added chambrage (the necking down of the chamber to the bore diameter).

Since a constant chamber volume was desired, chamber length had to change when chambrage was introduced. The chambrage was modeled as a truncated cone whose length was 76.2 mm, which required the chamber length be reduced from 776.22 mm to 541.02 mm, with the radius of the breech end of the chamber up to the beginning of the chambrage being 76.91 mm. Baseline and chambrage configurations are illustrated in Figure 6.

Flamespreading in XKTC is convectively driven, with the initial stimulus provided by some level of modeling of igniter functioning. In these calculation, the igniter was described as venting over the rear 304.8 mm of propellant bed, causing the entire propellant bed to be ignited within 2 ms. The resistance was modeled with a linearly interpolated table of travel versus resistive pressures. The resistance started at 0.690 MPa at 0-mm travel, remained constant for 6.35 mm, rose to 6.90 MPa at 12.70 mm, fell to 0.690 MPa at 19.05 mm and remained constant until barrel exit, as illustrated in Figure 7.

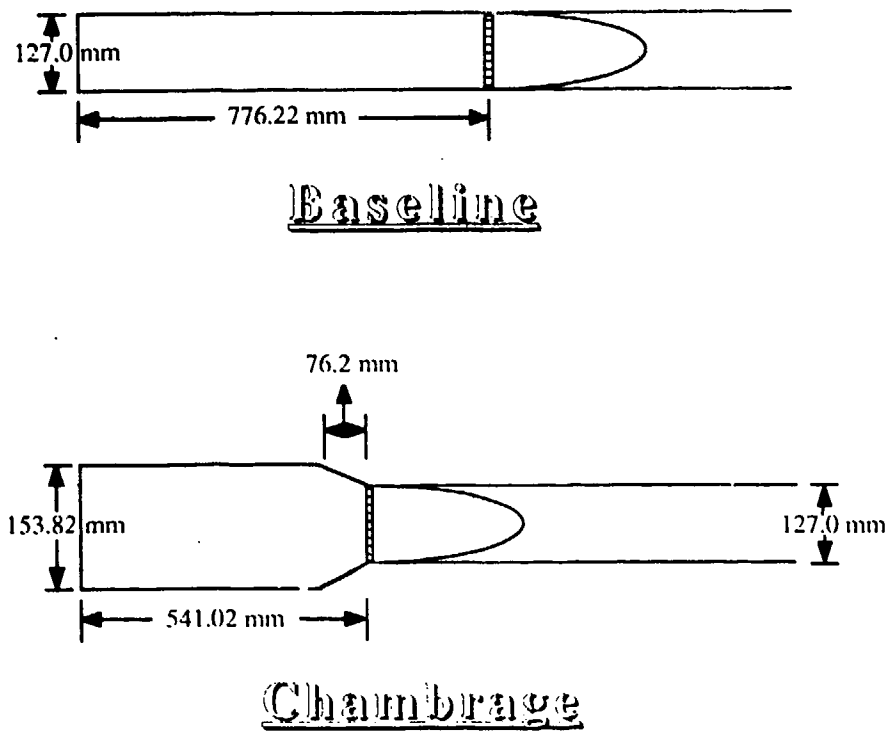

Figure 6. Baseline and Chambrage Configurations

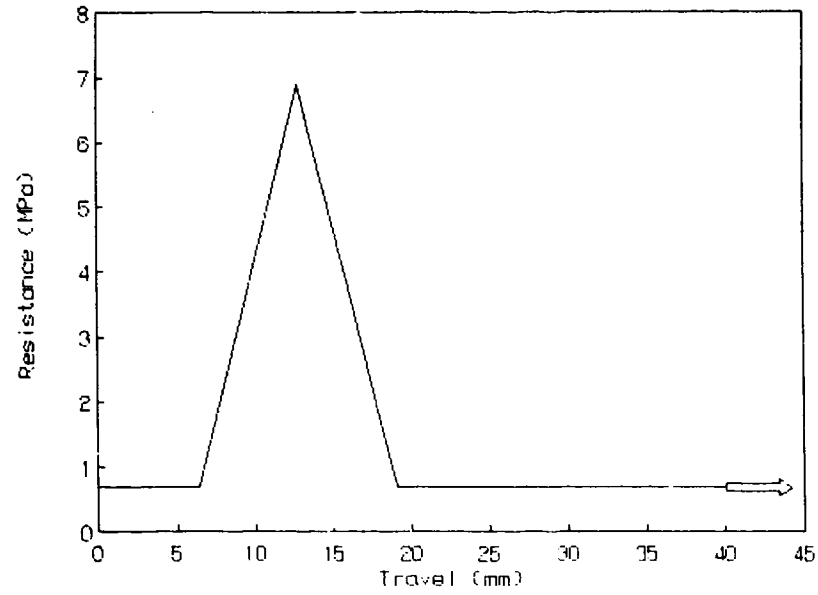

Figure 7. Barrel Resistance Profile

The results of this second series of calculations are given in Table 6. The propellant dimensions selected for these calculations were those determined to achieve a peak pressure of 345 MPa with XKTC, assuming zero barrel resistance, no chambrage and the propellant ignited at time zero for the given C/M.

Table 6. Comparisons of Calculated Maximum Breech Pressures and Muzzle Velocities for XKTC and IBHVG2

Code	Variation*	Maximum Breech Pressure (MPa)	Time (ms)	Muzzle Velocity (m/s)	Time (ms)	C/M
XKTC	B	345	6.5	1352	10.4	1.0
IBHVG2	B	346	6.3	1363	10.3	1.0
XKTC	R	363	6.5	1379	10.2	1.0
IBHVG2	R	365	6.3	1387	10.2	1.0
XKTC	F	332	6.0	1337	9.8	1.0
XKTC	C	310	6.5	1303	10.5	1.0
XKTC	FRC	321	6.0	1317	9.8	1.0
XKTC	B	345	11.2	779	18.1	0.25
IBHVG2	B	348	11.1	783	18.0	0.25
XKTC	R	363	11.2	792	17.9	0.25
IBHVG2	R	367	11.0	796	17.8	0.25
XKTC	F	347	9.3	779	16.2	0.25
XKTC	C	336	11.4	774	18.1	0.25
XKTC	FRC	351	9.7	784	16.5	0.25

* B = Baseline R = Resistance F = Flamespreading C = Chambrage

The first line of Table 6, the baseline calculation with XKTC, is the same as the XKTC calculation on the second line of Table 5. The second line of Table 6, the baseline IBHVG2 calculation, is also the same as that shown on the second line of Table 5. The next two lines result from adding bore resistance, and show the expected rise in peak pressure for both XKTC and IBHVG2. The following line results from adding just flamespreading to the XKTC baseline calculation and documents a drop in peak pressure. The next line represents adding just chambrage to the baseline XKTC calculation -- note the huge drop in peak pressure of 35 MPa! The final calculation in the C/M = 1.0 series has flamespreading, bore resistance, and chambrage added to the baseline data base. Again, the large decrease in peak pressure is attributed primarily to the chambrage.

For C/M of 0.25, it is seen that bore resistance makes a significant change, but about the same for both XKTC and IBHVG2. The influence of flamespreading and chambrage are about 2/5 as great as those for the higher C/M.

Plots of ratios of breech pressure to base pressure from the XKTC calculations for this second series of comparison calculations are found in Figure 8. Plot 25 results from having added flamespread alone to the baseline. Plot 26 has resistance added to the baseline. Neither Plot 25 nor Plot 26 shows much difference from the baseline plot. Plot 28 had added chambrage to the baseline; Plot 29 had added chambrage, flamespreading, and resistance. Both Plots 28 and 29 show a much lower pressure ratio at early time. Plots 27 and 30 are "full" XKTC simulations (which now include projectile intrusion into the chamber) of the inert case (Plot 27) and the caseless gun firings (Plot 28). The fact that the gradient curves in Figure 8 have assumed the general shape of the measured curves leads us to believe that the major interior ballistic parameters have now been included.

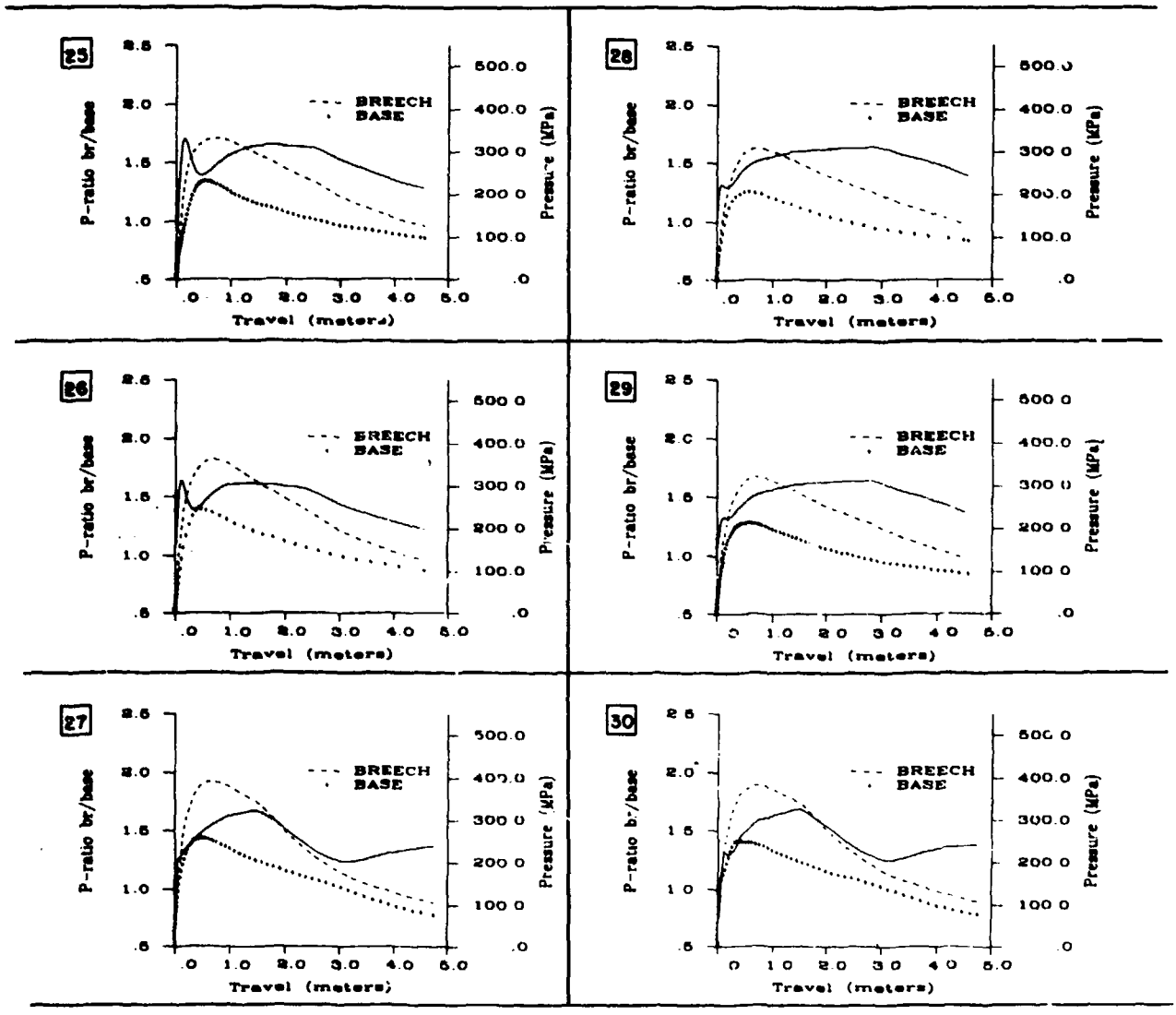

Figure 8. XKTC-Calculated Breech/Base Pressure Ratio Curves With Added Complexities.

V. DISCUSSION AND CONCLUSIONS

Earlier studies using the XKTC code[1] demonstrated that propellant packaging and boattail intrusion can have significant impact on maximum chamber pressures. The current investigation reveals that flamespreading and, to an even greater extent, chambrage, can affect calculated pressures as well, particularly at large C/M ratios.

In this study, we have seen that the presence of chambrage makes a significant difference in the pressure gradient. The larger cross section of the chamber results in a closer axial proximity of combustion product gases to the projectile base, with less axial motion and shorter transit times required to transfer pressures downbore. The result is a significant reduction in the pressure gradient, as shown in plots 28 and 29 of Figure 8.

The role of flamespreading, as well, has been demonstrated in this study. The phased ignition of propellant surfaces, rather than the simultaneous ignition event assumed in most lumped-parameter codes, can influence the overall rate of gas production, as well as the formation of pressure waves, resulting in differences in the inbore trajectory and impacting maximum chamber pressure. Wave dynamics associated with the rarefaction accompanying projectile motion may add further structure to the pressure gradient.

But a more interesting feature of the structure of the pressure gradient is shown in this study to accompany the formation of a region of axial ullage between the propellant charge and the projectile as it first moves downbore. XKTC calculations suggest that a lower gas pressure gradient exists in this single-phase region than in the two-phase region of the propellant charge, primarily because of a lower resistance to the transfer of pressure information. This result suggests that lumped-parameter codes might benefit from a two-region pressure gradient in order to capture the true structure of the pressure field. Such a feature might prove to be particularly important for simulation of stick charges, for which a well defined boundary between the two regions persists throughout the interior ballistic cycle, or for highly nonuniform initial distributions of propellant, as when firing low-zone artillery changes.

All of the above effects are exacerbated by an increase in C/M, since the projectile then moves out more rapidly, and axial dimensions and accompanying transit times are increased at a time when significant amounts of gas are still being locally produced in the gun chamber.

We conclude from this study that lumped-parameter interior ballistic codes could benefit greatly from the inclusion of a new or modified gradient equation including functional dependence on C/M, chambrage, propellant distribution and ullage; the influences of flamespreading and wave dynamics may also be included, though the basis for such terms would necessarily be more heuristic.

REFERENCES

1. F. W. Robbins, J. A. Kudzal, J. A. McWilliams and P. S. Gough, Experimental Determination of Stick Charge Flow Resistance", 17th JANNAF Combustion Meeting, CPIA Publication 329, Vol. II, pp. 97-118, November 1980.

2. F. W. Robbins and A. W. Horst, "Detailed Characterization of the Interior Ballistics of Slotted Stick Propellant", BRL-TR-2591, USA Ballistic Research Laboratory, Aberdeen Proving Ground, MD, September 1984. AD A147 499.

3. F. W. Robbins, A. A. Koszoru and T. C. Minor, "A Theoretical and Experimental Interior Ballistic Characterization of Combustible Cases", 9th International Symposium on Ballistics, Part 1, pp. 21-28, April 1986.

4. F. W. Robbins, "Comparison of TDNOVA Results with an Analytic Solution", ARBRL-MR-03299, USA ARRADCOM, Ballistic Research Laboratory, Aberdeen Proving Ground, MD, July 1983. AD A132 969.

5. R. D. Anderson and K. D. Fickie, "IBHVG2 -- A User's Guide," Technical Report BRL-TR-2829, US Army Ballistic Research Laboratory, Aberdeen Proving Ground, MD, July 1987. AD B117 104.

6. P. S. Gough, personal communication, September 1986.

APPENDIX A

XKTC Data Base

```
 GRADIENT  TESTS  600  IN~3  X6C05
TFFFTTT          1 1 0       00
   25    -3     0 3500
10.0        180.0       0.0001      2.0         0.05        0.01        0.0001      0.0001
  300   100  1100   100  1500   100
    6     0     0     5     0     0     1     2     0     0     0     8                     0
    0
529.         14.7        28.896      1.4
529.0
JA2  7PF  LOT  RH2-5      0.0          30.56       21.6        .06
    7    .500     0.020        1.25        7.
15000.       1.0         41754.                   .5
 8000.      .00030      1.000       100000.     .000300     1.000       0.0         520.
19826000.  23.0000     1.2300      27.00
0.0          2.5         4.00        2.5         6.0         2.5         21.9        2.5
23.37        2.5         210.56       2.5
 6.0          0.         6.25         0.         7.2          00.         7.8         0.
 210.56       0.
7.77         0.0228      0.7
 30.56       21.6        44.0        0.000
0.0          3.          12.         30.         40.         50.          80.         30.
```

APPENDIX B

IBHVG2 Data Base

```
$HEAT
      TSHL = 0.00450   CSHL = 1848    RSHL = 0.284
      TWAL = 293       HO = 0.0648    HL   = 1
$GUN
      NAME = '600 IN~ TEST'     CHAM = 600    TRAV = 180
      GRVE = 5.0     LAND = 5.0     G/L  = 1. TWST = 99
$PROJ
      NAME = 'FLAT'    PRWT = 21.6
$PDIS
      SHOW='PMAX'  DECK='OUT'
$PDIS
      SHOW='CHWT'  DECK='PROP'  NTH=2
$PDIS
      SHOW='DIAM'  DECK='PROP'  NTH=2
$PDIS
      SHOW='PD'  DECK='PROP'  NTH=2
$PDIS
      SHOW='WEB'  DECK='PROP'  NTH=2
$PDIS
      SHOW='VMUZ'  DECK='OUT'
$PDIS
      SHOW='ZMUZ(2)'  DECK='OUT'
$PDIS
      SHOW='LDEN'  DECK='OUT'
$RESI
      NPTS = 5   AIR  = 0
      TRAV = 0, .25, .5, .75, 180
      PRES = 0,  0,   0,   0,  0
$INFO
      RUN  = 'I6C05  '   DELT = 5E-5          DELP = 5E-5
      GRAD = 1           POPT = 1,1,1,0,2    SOPT = 0
      EPS  = 0.002       CONP = 0
$RECO
      NAME = 'NONE'   RECO = 0   RCWT = 0
$PRIM
      NAME = 'AIR'    CHWT = .01039   TEMP = 294
      GAMA = 1.4      FORC = 28284    COV  = 27

$PROP
      NAME = 'JA2  7P'      CHWT = 21.6       GRAN = '7PF'
      RHO  = 0.06           GAMA = 1.23       FORC = 380000
      COV  = 27.            TEMP = 3141       EROS = 0.0
      NTBL=-2               EX4L=1.,1.
      PR4L=8000,100000      CF4L=.0003,.0003
      LEN  = 1.25           DIAM = 0.50
      PD = 0.020            WEB=.11
```

DISTRIBUTION LIST

No. of Copies	Organization
12	Administrator Defense Technical Info Center ATTN: DTIC-FDAC Cameron Station, Bldg 5 Alexandria, VA 22304-6145
1	Commander USA Concepts Analysis Agency ATTN: D. Hardison 8120 Woodmont Avenue Bethesda, MD 20014-2797
1	HQDA/DAMA-ZA Washington, DC 20310-2500
1	HQDA, DAMA-CSM, Washington, DC 20310-2500
1	HQDA/SARDA Washington, DC 20310-2500
1	C.I.A. OIR/DB/Standard GE47 HQ Washington, D.C. 20505
1	Commander US Army War College ATTN: Library-FF229 Carlisle Barracks, PA 17013
1	US Army Ballistic Missile Defense Systems Command Advanced Technology Center P. O. Box 1500 Huntsville, AL 35807-3801
1	Chairman DOD Explosives Safety Board Room 856-C Hoffman Bldg. I 2461 Eisenhower Avenue Alexandria, VA 22331-9999
1	Commander US Army Materiel Command ATTN: AMCPM-GCM-WF 5001 Eisenhower Avenue Alexandria, VA 22333-5001
1	Commander US Army Materiel Command ATTN: AMCDRA-ST 5001 Eisenhower Avenue Alexandria, VA 22333-5001
1	Commander US Army Materiel Command ATTN: AMCDE-DW 5001 Eisenhower Avenue Alexandria, VA 22333-5001

No. of Copies	Organization
5	Project Manager Cannon Artillery Weapons System, ARDC, AMCCOM ATTN: AMCPM-CW, AMCPM-CWW AMCPM-CWS M. Fisette AMCPM-CWA H. Hassmann AMCPM-CWA-S R. DeKleine Dover, NJ 07801-5001
2	Project Manager Munitions Production Base Modernization and Expansion ATTN: AMCPM-PBM, A. Siklosi AMCPM-PBM-E, L. Laibson Dover, NJ 07801-5001
3	Project Manager Tank Main Armament System ATTN: AMCPM-TMA, K. Russell AMCPM-TMA-105 AMCPM-TMA-120 Dover, NJ 07801-5001
1	Commander US Army Watervliet Arsenal ATTN: SARWV-RD, R. Thierry Watervliet, NY 12189-5001
1	Commander U.S. Army ARDEC ATTN: SMCAR-MSI Dover, NJ 07801-5001
1	Commander U.S. Army ARDEC ATTN: SMCAR-TDC Dover, NJ 07801-5001
4	Commander US Army Armament Munitions and Chemical Command ATTN: AMSMC-IMP-L Rock Island, IL 61299-7300
1	HQDA DAMA-ART-M Washington, DC 20310-2500
1	Commander US Army AMCCOM ARDEC CCAC ATTN: SMCAR-CCB-TL Benet Weapons Laboratory Watervliet, NY 12189-4050

DISTRIBUTION LIST

No. of Copies	Organization
3	Commander US Army ARDEC ATTN: SMCAR-MSI SMCAR-TDC SMCAR-LC LTC N. Barron Dover, NJ 07801-5001
7	Commander US Army ARDEC ATTN: SMCAR-LCA A. Beardell D. Downs S. Finstein S. Westley S. Bernstein C. Roller J. Rutkowski Dover, NJ 07801-5001
3	Commander US Army ARDEC ATTN: SMCAR-LCB-I D. Spring SMCAR-LCE SMCAR-LCM-E S. Kaplowitz Dover, NJ 07801-5001
4	Commander US Army ARDEC ATTN: SMCAR-LCS SMCAR-LCU-CT E. Barrieres R. Davitt SMCAR-LCU-CV C. Mandala Dover, NJ 07801-5001
3	Commander US Army ARDEC ATTN: SMCAR-LCW-A M. Salsbury SMCAR-SCA L. Stiefel B. Brodman Dover, NJ 07801-5001
1	Commander US Army Aviation Systems Command ATTN: AMSAV-ES 4300 Goodfellow Blvd. St. Louis, MO 63120-1798
1	Director US Army Aviation Research and Technology Activity Ames Research Center Moffett Field, CA 94035-1099
1	Commander US Army Communications - Electronics Command ATTN: AMSEL-ED Fort Monmouth, NJ 07703-5301
1	Commander CECOM R&D Technical Library ATTN: AMSEL-M-L (Report Section) B.2700 Fort Monmouth, NJ 07703-5000
1	Commander US Army Harry Diamond Lab. ATTN: DELHD-TA-L 2800 Powder Mill Road Adelphi, MD 20783-1145
1	Commander US Army Missile and Space Intelligence Center ATTN: AIAMS-YDL Redstone Arsenal, AL 35898-5500
1	Commander US Army Missile Command Research, Development, and Engineering Center ATTN: AMSMI-RD Redstone Arsenal, AL 35898-5245
1	Commandant US Army Aviation School ATTN: Aviation Agency Fort Rucker, AL 36360
1	Commander US Army Tank Automotive Command ATTN: AMSTA-TSL Warren, MI 48397-5000
1	Commander US Army Tank Automotive Command ATTN: AMSTA-CG Warren, MI 48397-5000
1	Project Manager Improved TOW Vehicle ATTN: AMCPM-ITV US Army Tank Automotive Command Warren, MI 48397-5000

DISTRIBUTION LIST

No. of Copies	Organization
2	Program Manager M1 Abrams Tank System ATTN: AMCPM-GMC-SA, T. Dean Warren, MI 48092-2498
1	Project Manager Fighting Vehicle Systems ATTN: AMCPM-FVS Warren, MI 48092-2498
1	President US Army Armor & Engineer Board ATTN: ATZK-AD-S Fort Knox, KY 40121-5200
1	Project Manager M-60 Tank Development ATTN: AMCPM-M60TD Warren, MI 48092-2498
1	Director US Army TRADOC Systems Analysis Activity ATTN: ATOR-TSL White Sands Missile Range, NM 88002
1	Commander US Army Training & Doctrine Command ATTN: ATCD-MA/ MAJ Williams Fort Monroe, VA 23651
2	Commander US Army Materials and Mechanics Research Center ATTN: AMXMR-ATL Tech Library Watertown, MA 02172
1	Commander US Army Research Office ATTN: Tech Library P. O. Box 12211 Research Triangle Park, NC 27709-2211
1	Commander US Army Belvoir Research and Development Center ATTN: STRBE-WC Fort Belvoir, VA 22060-5606
1	Commander US Army Logistics Mgmt Ctr Defense Logistics Studies Fort Lee, VA 23801
1	Commandant US Army Infantry School ATTN: ATSH-CD-CS-OR Fort Benning, GA 31905-5400
1	Commandant US Army Command and General Staff College Fort Leavenworth, KS 66027
1	Commandant US Army Special Warfare School ATTN: Rev & Tng Lit Div Fort Bragg, NC 28307
3	Commander Radford Army Ammunition Plant ATTN: SMCRA-QA/HI LIB Radford, VA 24141-0298
1	Commander US Army Foreign Science & Technology Center ATTN: AMXST-MC-3 220 Seventh Street, NE Charlottesville, VA 22901-5396
2	Commandant US Army Field Artillery Center & School ATTN: ATSF-CO-MW, B. Willis Ft. Sill, OK 73503-5600
1	Commander US Army Development and Employment Agency ATTN: MODE-ORO Fort Lewis, WA 98433-5099
1	Office of Naval Research ATTN: Code 473, R. S. Miller 800 N. Quincy Street Arlington, VA 22217-9999
3	Commandant US Army Armor School ATTN: ATZK-CD-MS M. Falkovitch Armor Agency Fort Knox, KY 40121-5215
2	Commander Naval Sea Systems Command ATTN: SEA 62R SEA 64 Washington, DC 20362-5101

DISTRIBUTION LIST

No. of Copies	Organization
1	Commander Naval Air Systems Command ATTN: AIR-954-Tech Lib Washington, DC 20360
1	Assistant Secretary of the Navy (R, E, and S) ATTN: R. Reichenbach Room 5E787 Pentagon Bldg. Washington, DC 20350
1	Naval Research Lab Tech Library Washington, DC 20375
5	Commander Naval Surface Weapons Center ATTN: Code G33, J. L. East W. Burrell J. Johndrow Code G23, D. McClure Code DX-21 Tech Lib Dahlgren, VA 22448-5000
2	Comander US Naval Surface Weapons Center ATTN: J. P. Consaga C. Gotzmer Indian Head, MD 20640-5000
4	Commander Naval Surface Weapons Center ATTN: S. Jacobs/Code 240 Code 730 K. Kim/Code R-13 R. Bernecker Silver Spring, MD 20903-5000
2	Commanding Officer Naval Underwater Systems Center Energy Conversion Dept. ATTN: CODE 5B331, R. S. Lazar Tech Lib Newport, RI 02840
5	Commander Naval Weapons Center ATTN: Code 388, R. L. Derr C. F. Price T. Boggs T. Parr Info. Sci. Div. China Lake, CA 93555-6001
2	Superintendent Naval Postgraduate School Dept. of Mech. Engineering Monterey, CA 93943-5100
1	Program Manager AFOSR Directorate of Aerospace Sciences ATTN: L. H. Caveny Bolling AFB, DC 20332-0001
6	Commander Naval Ordnance Station ATTN: P. L. Stang L. Torreyson T. C. Smith D. Brooks W. Vienna Tech Library Indian Head, MD 20640-5000
1	AFSC/SDOA Andrews AFB, MD 20334
3	AFRPL/DY, Stop 24 ATTN: J. Levine/DYCR R. Corley/DYC D. Williams/DYCC Edwards AFB, CA 93523-5000
1	AF Astronautics Laboratory AFAL/TSTL (Technical Library) Edwards AFB, CA 93523-5000
1	AFATL/DLYV Eglin AFB, FL 32542-5000
1	AFATL/DLXP Eglin AFB, FL 32542-5000
1	AFATL/DLJE Eglin AFB, FL 32542-5000
1	AFATL/DOIL ATTN: (Tech Info Center) Eglin AFB, FL 32542-5438
1	NASA/Lyndon B. Johnson Space Center ATTN: NHS-22, Library Section Houston, TX 77054
1	AFELM, The Rand Corporation ATTN: Library D 1700 Main Street Santa Monica CA 90401-3297
2	AAI Corporation ATTN: J. Hebert J. Frankle D. Cleveland P. O. Box 6767 Baltimore, MD 21204

DISTRIBUTION LIST

No. of Copies	Organization
1	Aerojet Ordnance Company ATTN: D. Thatcher 2521 Michelle Drive Tustin, CA 92680-7014
1	Aerojet Solid Propulsion Co. ATTN: P. Micheli Sacramento, CA 95813
1	Atlantic Research Corporation ATTN: M. K. King 5390 Cheorokee Avenue Alexandria, VA 22312-2302
1	AVCO Everett Rsch Lab ATTN: D. Stickler 2385 Revere Beach Parkway Everett, MA 02149-5936
2	Calspan Corporation ATTN: C. Morphy P. O. Box 400 Buffalo, NY 14225-0400
1	General Electric Company Armament Systems Dept. ATTN: M. J. Bulman, Room 1311 128 Lakeside Avenue Burlington, VT 05401-4985
1	IITRI ATTN: M. J. Klein 10 W. 35th Street Chicago, IL 60616-3799
1	Hercules Inc. Allegheny Ballistics Laboratory ATTN: R. B. Miller P. O. Box 210 Cumberland, MD 21501-0210
1	Hercules, Inc. Bacchus Works ATTN: K. P. McCarty P. O. Box 98 Magna, UT 84044-0098
1	Hercules, Inc. Radford Army Ammunition Plant ATTN: J. Pierce Radford, VA 24141-0299
1	Lawrence Livermore National Laboratory ATTN: L-355, A. Buckingham M. Finger P. O. Box 808 Livermore, CA 94550-0622
1	Lawrence Livermore National Laboratory ATTN: L-324/M. Constantino P. O. Box 808 Livermore, CA 94550-0622
1	Olin Corporation Badger Army Ammunition Plant ATTN: R. J. Thiede Baraboo, WI 53913
1	Olin Corporation Smokeless Powder Operations ATTN: D. C. Mann P.O. Box 222 St. Marks, FL 32355-0222
1	Paul Gough Associates, Inc. ATTN: P. S. Gough P. O. Box 1614, 1048 South St. Portsmouth, NH 03801-1614
1	Physics International Company ATTN: Library H. Wayne Wampler 2700 Merced Street San Leandro, CA 94577-5602
1	Princeton Combustion Research Lab., Inc. ATTN: M. Summerfield 475 US Highway One Monmouth Junction, NJ 08852-9650
2	Rockwell International Rocketdyne Division ATTN: BA08 J. E. Flanagan J. Gray 6633 Canoga Avenue Canoga Park, CA 91303-2703
1	Science Applications, Inc. ATTN: R. B. Edelman 23146 Cumorah Crest Drive Woodland Hills, CA 91364-3710
3	Thiokol Corporation Huntsville Division ATTN: D. Flanigan R. Glick Tech Library Huntsville, AL 35807
2	Thiokol Corporation Elkton Division ATTN: R. Biddle Tech Lib. P. O. Box 241 Elkton, MD 21921-0241

DISTRIBUTION LIST

No. of Copies	Organization
1	Veritay Technology, Inc. ATTN: E. Fisher 4845 Millersport Hwy. P. O. Box 305 East Amherst, NY 14051-0305
1	Universal Propulsion Company ATTN: H. J. McSpadden Black Canyon Stage 1 Box 1140 Phoenix, AZ 85029
1	Battelle Memorial Institute ATTN: Tech Library 505 King Avenue Columbus, OH 43201-2693
1	Brigham Young University Dep of Chemical Engineering ATTN: M. Beckstead Provo, UT 84601
1	California Institute of Tech 204 Karman Lab Main Stop 301-46 ATTN: F. E. C. Culick 1201 E. California Street Pasadena, CA 91109
1	California Institute of Tech Jet Propulsion Laboratory ATTN: L. D. Strand 4800 Oak Grove Drive Pasadena, CA 91109-8099
1	University of Illinois Dept of Mech/Indust Engr ATTN: H. Krier 144 MEB; 1206 N. Green St. Urbana, IL 61801-2978
1	University of Massachusetts Dept. of Mech. Engineering ATTN: K. Jakus Amherst, MA 01002-0014
1	University of Minnesota Dept. of Mech. Engineering ATTN: E. Fletcher Minneapolis, MN 55414-3368
1	Case Western Reserve University Division of Aerospace Sciences ATTN: J. Tien Cleveland, OH 44135
3	Georgia Institute of Tech School of Aerospace Eng. ATTN: B. T. Zinn E. Price W. C. Strahle Atlanta, GA 30332
1	Institute of Gas Technology ATTN: D. Gidaspow 3424 S. State Street Chicago, IL 60616-3896
1	Johns Hopkins University Applied Physics Laboratory Chemical Propulsion Information Agency ATTN: T. Christian Johns Hopkins Road Laurel, MD 20707-0690
1	Massachusetts Institute of Technology Dept of Mechanical Engineering ATTN: T. Toong 77 Massachetts Avenue Cambridge, MA 02139-4307
1	G. M. Faeth Pennsylvania State University Applied Research Laboratory University Park, PA 16802-7501
1	Pennsylvania State University Dept. of Mech. Engineering ATTN: K. Kuo University Park, PA 16802-7501
1	Purdue University School of Mechanical Engineering ATTN: J. R. Osborn TSPC Chaffee Hall West Lafayette, IN 47907-1199
1	SRI International Propulsion Sciences Division ATTN: Tech Library 333 Ravenswood Avenue Menlo Park, CA 94025-3493
1	Rensselaer Polytechnic Inst. Department of Mathematics Troy, NY 12181

DISTRIBUTION LIST

No. of Copies	Organization
2	Director Los Alamos Scientific Lab ATTN: T3, D. Butler M. Division, B. Craig P. O. Box 1663 Los Alamos, NM 87544
1	Stevens Institute of Technology Davidson Laboratory ATTN: R. McAlevy, III Castle Point Station Hoboken, NJ 07030-5907
1	Rutgers University Dept. of Mechanical and Aerospace Engineering ATTN: S. Temkin University Heights Campus New Brunswick, NJ 08903
1	University of Southern California Mechanical Engineering Dept. ATTN: 0HE200, M. Gerstein Los Angeles, CA 90089-5199
2	University of Utah Dept. of Chemical Engineering ATTN: A. Baer G. Flandro Salt Lake City, UT 84112-1194
1	Washington State University Dept. of Mech. Engineering ATTN: C. T. Crowe Pullman, WA 99163-5201

Aberdeen Proving Ground

Dir, USAMSAA
ATTN: AMXSY-D
AMXSY-MP, H. Cohen

Cdr, USATECOM
ATTN: AMSTE-SI-F
AMSTE-CM-F, L. Nealley

Cdr, CSTA
ATTN: STECS-AS-H, R. Hendricksen

Cdr, CRDC, AMCCOM
ATTN: SMCCR-RSP-A
SMCCR-MU
SMCCR-SPS-IL

USER EVALUATION SHEET/CHANGE OF ADDRESS

This Laboratory undertakes a continuing effort to improve the quality of the reports it publishes. Your comments/answers to the items/questions below will aid us in our efforts.

1. BRL Report Number_____ Date of Report_____

2. Date Report Received_____

3. Does this report satisfy a need? (Comment on purpose, related project, or other area of interest for which the report will be used.)_____

_____

_____

4. How specifically, is the report being used? (Information source, design data, procedure, source of ideas, etc.)_____

_____

_____

5. Has the information in this report led to any quantitative savings as far as man-hours or dollars saved, operating costs avoided or efficiencies achieved, etc? If so, please elaborate._____

_____

_____

6. General Comments. What do you think should be changed to improve future reports? (Indicate changes to organization, technical content, format, etc.)

_____

_____

_____

CURRENT ADDRESS

_____
Name

_____
Organization

_____
Address

_____
City, State, Zip

7. If indicating a Change of Address or Address Correction, please provide the New or Correct Address in Block 6 above and the Old or Incorrect address below.

OLD ADDRESS

_____
Name

_____
Organization

_____
Address

_____
City, State, Zip

(Remove this sheet, fold as indicated, staple or tape closed, and mail.)